Nuclear Instruments and Methods 192 (1982) 375–378
North-Holland Publishing Company

A SIMPLE ADC UNIT FOR COSMIC RAY AIR SHOWER EXPERIMENTS

G.C. GOSWAMI, B. GHOSH, M.R. GHOSHDASTIDAR, S.K. SENGUPTA and N. CHAUDHURI
Department of Physics, University of North Bengal, Darjeeling, India

Received 10 November 1980 and in revised form 14 April 1981

The design of a new low cost analog-to-digital converter system is described. It is based upon the method of linearising the charging process of a storage condenser and is controlled by logic gates. Its tested characteristics have been found to be reliable for application in cosmic ray air shower experiments.

1. Introduction

The digital encoding of pulse height in nuclear pulse techniques with the method of Wilkinson [1] for digital measurements has succeeded over some other methods for digitisation of analog pulses. Manfredy and Rimini [2], among others, have described a Wilkinson type analog-to-digital converter (ADC) based upon the method of linearisation of the discharging process of a storage condenser. The method of Wilkinson has been used in the present work to design a new analog-to-digital converter based upon the technique of linearising the charging process of a condenser for use in nuclear physics and cosmic ray air shower experiments. The design, operation and performance of the converter are described in this paper.

2. Principle of operation

The operation of the converter starts with the charging of a condenser by means of a constant current source (linear ramp generator) to a voltage equal to the input pulse amplitude to be measured. The charging time of the condenser to a voltage equal to the input voltage is measured by means of a 1 MHz clock pulse. The operating principle is indicated in fig. 1. As the condenser voltage rises linearly to the input voltage, the number of clock pulses counted during the capacitor charging time is therefore proportional to the input voltage. The new design for the realisation of the converter is described in the following section.

3. Description of the converter circuit

The circuit diagram of the converter is shown in fig. 2. The whole circuit consists of two parts: (1) the ADC consisting of four operational amplifiers, two silicon transistors (T_1, T_2) and two TTL ICs (IC-5, IC-6), (2) a built-in-programmer consisting of logic gates and counters indicated in fig. 2.

In the ADC circuit the transistor T_1 acts as a constant current source to charge the capacitor C connected to the collector of T_1 and T_2. The voltage follower IC-1 connected to the capacitor C is meant to give information about the voltage across C to the comparator IC-3. The transistor T_2 acts as an analog switch across the capacitor C.

The analog input pulse is fed to the comparator through a summing amplifier, the inverting input of the amplifier is connected to a preset for setting the output of the comparator at a zero logic level when the input voltage is at zero level. This occurs due to low voltage on the collector of T_2 in the conducting state. The output voltage of the comparator IC-3 is clipped at a high logic level and connected to the input of an inverting logic gate G_1. The output of the inverter is connected to the "reset to zero" (R_0) input of a decade counter, IC-6. The output of G_1 is further inverted by G_2 and then applied to one of the inputs of the trigger controlling gate G_3. This input, directly related to the voltage setting time of the analog multiplexer, will not allow any start pulse to the ADC until the voltage is set for scanning. The output of the gate G_3 is connected to the "Rest to Nine" (R_9) input of IC-6 whose outputs Q_A and Q_D are used to control the ramp generator as these two

0029-554X/82/0000–0000/$02.75

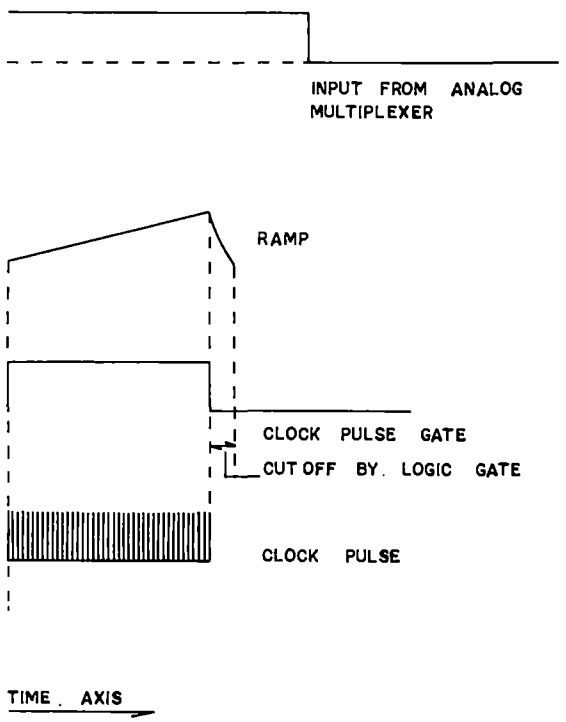

Fig. 1. Principle of the ADC.

change their logic states with R_0 and R_9. Here decade counter (IC-6) is used for "preset' and "clear" purposes. Any flip-flop with "preset" and "clear" can be used instead of IC-6. But such a flip-flop should be properly gated to that when any one of "preset" and "clear" goes low the other should remain high. But in case of decade counter no such gate is necessary. The output Q_D of the IC-6 is connected to one of the inputs of the Schmidt trigger IC-5 containing a 1 MHz clock pulse and also the inverting input of the high speed operational amplifier IC-4 of unit gain. Instead of a Schmidt trigger (IC-5) a simple AND gate can be used provided the input 1 MHz clock is a Schmidt triggered output to avoid errors that may occur in the counters which follow the ADC and which are very susceptible to noise. The output of IC-4 is connected to the base of T_2. The noninverting input of IC-4 is connected to a 10 kΩ resistor preset to apply a posi- of IC-11 is used to reset the analog multiplexer, T_2 goes negative and when Q_D is low the base of T_2 goes positive just to make T_2 conducting. The output of IC-5 gives the serial data output which can be connected to counters for parallel data output.

The built-in programme is an assembly of different logic gates (G_3–G_9), counters (IC-9 to IC-12) and

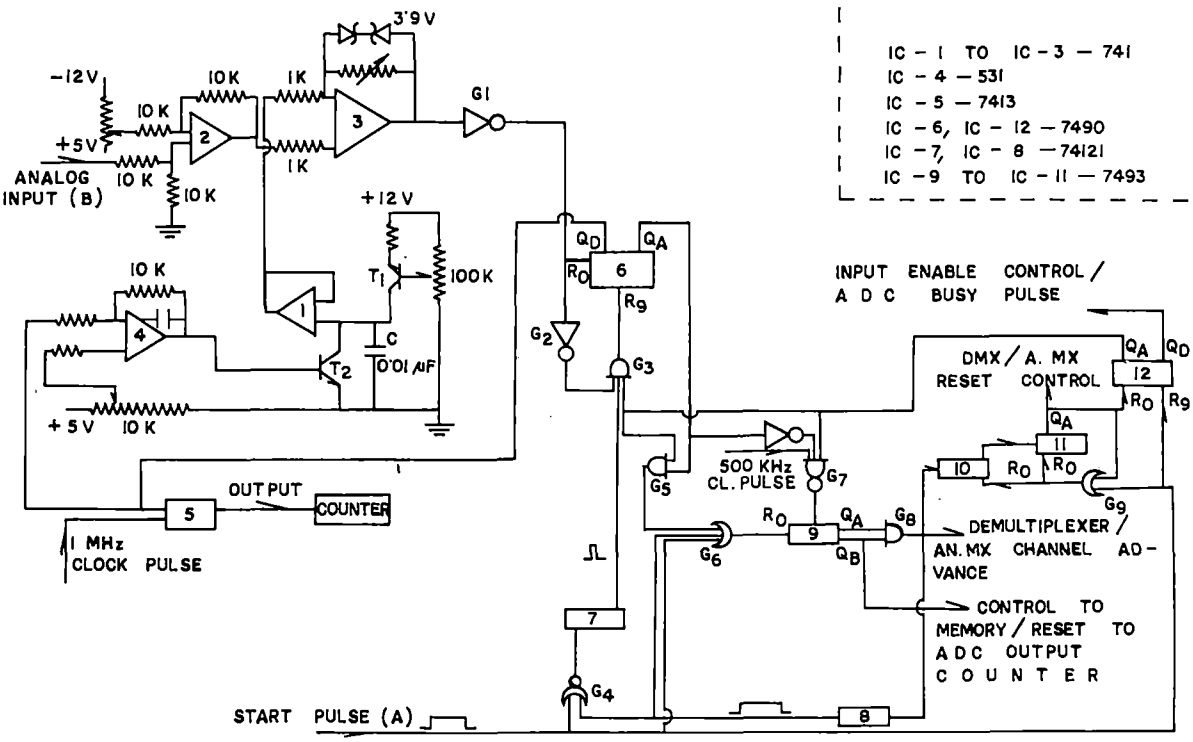

Fig. 2. Circuit diagram of the converter.

monostable multivibrators (IC-7, IC-8). The monostable multivibrator IC-7 triggers the ADC and IC-8 allows the voltage setting time of the analog multiplexer. For analysis with 16 channels, the output Q_A of IC-11 is used to reset the analog multiplexer, demultiplexer address register, the preset counters (IC-10 and IC-11) and programme controller IC-12.

4. Operation of the circuit

The unit IC-12 which controls the whole programme is normally reset to zero when the ADC will not scan any input voltage applied at the analog input terminal B. Whenever there is an input voltage, a positive start pulse derived from the control unit of the system where this ADC is intended to be used, is applied to the "start pulse" input terminal A. The width of the start pulse is slightly greater than the voltage setting time of the analog multiplexer with its output point connected to the analog input terminal B. The positive edge of the start pulse resets the IC-12 to nine (R_9) and IC-9, IC-10 and IC-11 to zero (R_0) through gates G_6 and G_9. The output Q_D of IC-12 after being inverted connects the analog multiplexer and demultiplexer to the ADC through "input enable control" and the output Q_A of IC-12 sets one of the inputs of gates G_3 and G_7 high. The input voltage makes the comparator IC-3 output high making R_0 of IC-6 low. The IC-7 is triggered at the end of the start pulse to reset IC-6 to nine (R_9) so that Q_A and Q_D of IC-6 are high. The width of the triggering pulse must be less than 1 μs for 1 MHz clock pulse. The output Q_D makes the base of T_2 negative and opens the 1 MHz clock pulse to the ADC counter and the storage capacitor starts charging at a constant current via T_1 until the output of comparator IC-3 goes to zero logic level making R_0 of IC-6 high. As R_0 of IC-6 goes high, the output Q_D of IC-6 becomes low stopping the 1 MHz clock pulse to the counters and making the base of T_2 positive to enable the capacitor C to discharge. Here the transistor T_2 is switched on and off by an operational amplifier (IC-4) but not by conventional TTL levels. This is done for the reason that logic low levels sometimes give ~0.1 V or even ~0.2 V. It is observed that there is a low conduction current through the transistor T_2 which affects the linearity between the digital output and the analog input. Replacing T_2 by a field effect transistor (FET) BFW 11 gives better result. With BFW 11 the gain of IC-4 is made about 3 so that when Q_D of IC-6 is low the gate of BFW 11 goes to about 1 V and when Q_D is high the gate goes to less than –4 V which is equal to the drain current cut-off voltage for BFW 11. At the end of the conversion the discharge of the capacitor C takes place through the FET. The FET being a better electronic switch than a silicon transistor, the discharge of the capacitor C is very fast to make the ADC ready for the next scan. The output Q_A of IC-6 being low, the output of G_5 is low. As there is no start pulse either at the input B or from IC-8, the output of G_6 is also low, making R_0 of IC-9 low. The 500 kHz clock pulse now enters the counter IC-9. The outputs Q_A and Q_B of IC-9 through G_8 increase the preset counter reading and the analog multiplexer and demultiplexer channel address by unity and produce another start pulse at the monostable multivibrator IC-8. As soon as the start pulse is generated, R_0 of IC-9 goes high through G_6 and the 500 kHz clock pulse entry to IC-9 is cut off starting a new cycle of operation. At the end of the sixteenth cycle, the output Q_A of IC-11 goes high, thus resetting the preset counter and the programme controlling IC-12 to zero, making the whole system ready for a new cycle of operations.

5. Discussion

The circuit described above has been operated for a long time and is now standardised for use in cosmic ray air shower experiments. The voltage ramp of the linear ramp generator has been photgraphed in a large number of test operations. The ramp has a fairly constant slope and good linearity up to 10 V. For a charging current corresponding to 10 mV/μs, the differential non-linearity is $<\pm 1\%$ for an input voltage higher than 50 mV but less than 10 V. Non-linearity above 10 V and can be achieved by operating the transistor T_1 with a higher voltage (15 V).

As 1 MHz quartz oscillator is used in the test circuit. The clock oscillator and the ramp generator are controlled by logic gates and hence all possible errors at small input voltages are expected to be negligible. Since R_9 overrides R_0, there may be an inaccuracy at zero input voltage of one channel width if the start pulse to IC-6 synchronises with the high logic level of the clock pulse. This can be avoided by interchanging "reset to nine" (R_9) with "reset to zero" (R_0) and by inverting outputs Q_A and Q_D of IC-6.

Fig. 3 shows the relation between the digital output and the analog input. The digital output of the

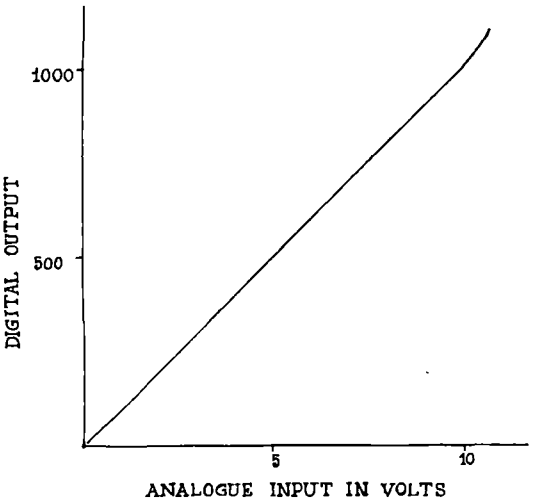

Fig. 3. Relation between the digital output and the analog input.

ADC for a particular height of an analog pulse is not constant but can be adjusted. To fix the digital output at a particular value the bias of the transistor T_1 is adjusted which controls the charging rate of the capacitor C. For a digital output 100 per volt with 1 MHz clock pulse the conversion time is 100 μs/V, But using a 10 MHz clock and adjusting the digital output 100 per volt the conversion time becomes 10 μs/V. In both cases the resolution is 10 mV. This resolution can be made 1 mV by making the digital output 1000 per volt by adjusting the charging rate of the capacitor C through transistor T_1. In this case the conversion time becomes 100 μs/V using a 10 MHz clock pulse. It may be mentioned that all operational amplifiers 741 should be replaced by 715. This is the main advantage of the ADC where we can adjust the conversion time and resolution according to need. The cost of the built-up ADC is at the level of one hundred rupees. The cost of similar such indigeneous ADCs is higher by at least a factor of four.

The authors acknowledge the provision of facilities including UGC Teacher Fellowships to G.C. Goswami, M.R. Ghoshdastidar and S.K. Sengupta and UGC Research Fellowship to B. Ghosh through the University of North Bengal, India.

The financial assistance received from the Department of Atomic Energy, Govt. of India is thankfully acknowledged.

References

[1] D.H. Wilkinson, Proc. Cambridge Phil. Soc. 46 (1950) 508.

[2] F.F. Manfredi and A. Rimini, NAS-NRC Publ. 1184 (1964) p. 186.

Nuclear Instruments and Methods 199 (1982) 505–507
North-Holland Publishing Company

A SAMPLE–HOLD AND ANALOG MULTIPLEXER FOR MULTIDETECTOR SYSTEMS

G.C. GOSWAMI, M.R. GHOSHDOSTIDAR, B. GHOSH and N. CHAUDHURI
Department of Physics, North Bengal University, Darjeeling-734430, India

Received 1 June 1981 and in revised form 20 November 1981

A new sample–hold circuit with an analog multiplexer system is described. Designed for multichannel acquistion of data from an air shower array, the system is being used for accurate measurements of pulse heights from 16 channels by the use of a single ADC.

1. Introduction

There are various ways of realising sample-and-hold circuits and the analog multiplexer systems (e.g. refs. 1–5). In all cases detection of each peak for monitoring during sampling and holding the peak of selected pulses and then feeding it to an ADC through an analog multiplexer by controlling a logic state is not provided. In the present design, peak detection, holding and monitoring the channels are simultaneously made by means of a simple circuit. The circuit in its new form is always adjustable both for holding time of the peak during sampling and closing the input lines after a definite interval of time or instantaneously. Realisation of the analog multiplexer is made simply by FET switches operated by operational amplifiers and TTL ICs.

2. Principle of operation

Charging a storage capacitor up to a voltage equal to the peak of the analog pulse by means of a conventional peak detector, used in almost all cases of analog peak detection in analog systems, is utilised in the working principle of the sample-and-hold circuit. The voltage across the capacitor is retained for a few microseconds and then allowed to discharge through a switch for sampling. A "Hold" command cuts off the discharging path of the capacitor and the input line. This "Hold" command further connects the analog multiplexer consisting of FET switches and operated by logic pulses to the output of sample-and-hold units for scanning with an ADC.

3. Description of the circuit

The circuit diagram for the system is shown in fig. 1. The whole circuit is composed of two parts,

(1) sample and hold (S–H) comprising operational amplifiers (Op Amp IC-1 to IC-3), TTL ICs (IC-6 and IC-7), two field effect transistors (FET) T_1 and T_3, and a silicon transistor T_2 for each channel together with an Op Amp (IC-4) and TTC ICs (IC-8 and IC-9) for general control of all the input lines;

(2) analog multiplexer comprising TTL ICs (IC-10, IC-11) for channel address and decoding and an Op Amp (IC-5) together with a FET (T_4) and a diode to switch "ON" and "OFF" for each channel.

For each channel the analog pulse is fed to a peak detector unit consisting of an Op Amp (IC-1), a diode and a capacitor C and to the base of the transistor T_2 through a 10 kΩ resistor. The drain of T_1, acting as an input switch, is connected to the input line. Transistor T_2, acting as a logic level clipper, is to operate IC-6 with the input pulse. Transistor T_3 operated by IC-3 acts as a switch to discharge the capacitor C by triggering IC-7 after a definite time from the arrival of a pulse controlled by the pulse width of IC-6. The triggering of IC-7 is controlled by connecting the 'S–H command' to the reset input. The output of the S–H unit is taken by a voltage follower (IC-2).

The drain of the transistor T_4 acting as the first channel input of the analog multipexer unit is connected to the output of the S–H unit and to the gate of T_4 by a 120 kΩ resistor. The gate is connected to the output of a high slew rate Op Amp (IC-5) through a forward diode. A small voltage, about 1 V, is applied to the non-inverting input so that when the output of IC-10 is low the gate of T_4 goes to drain voltage and when the output is high the gate goes beyond the drain current cut-off value switching off the input output line. All the source terminals of the FET switches operating in the position T_4 for 16 channels are shorted to give the output. The sequential connection of the channnels is obtained by decoding the channel address with IC-10 generated by IC-11 which contains a channel advance instruction at the C_p input. R_D of IC-7, enable control (E) of IC-10. and R_0 of IC-11 are held high during

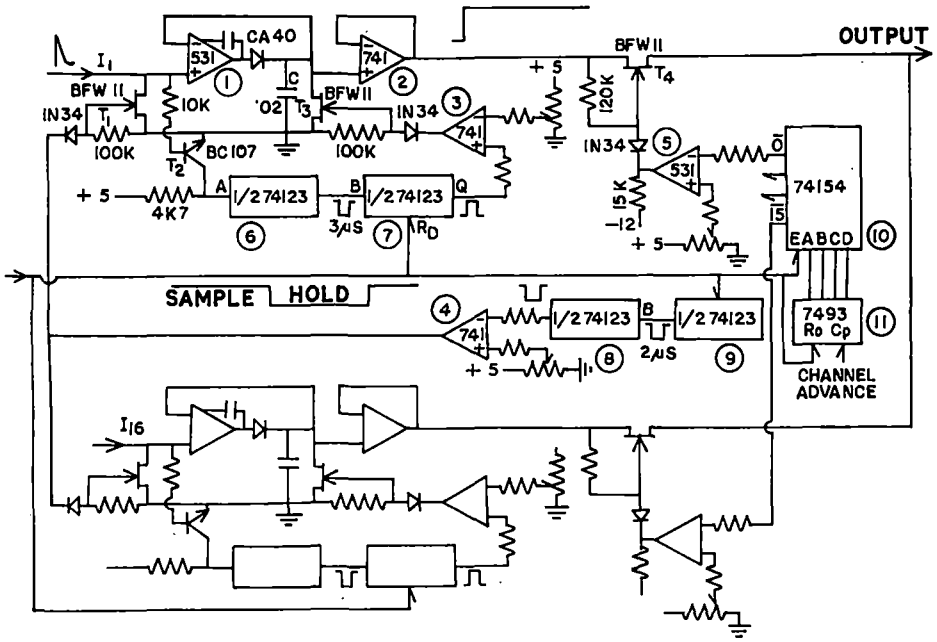

Fig. 1. Circuit diagram of sample-and-hold and analog multiplexer unit.

sampling and low on giving a "hold" command which closes the input line after 2 μs by operating IC-4 which makes the transistor T_1 conducting. The Q output of IC-6 of all the channels may be multiplexed and connected to a 7-segment LED display for monitoring (not shown in fig. 1).

4. Operation of the circuit

Analog pulses to be analysed coming from 16 detecting units are applied to the inputs I_1–I_{16}. Any analog pulse at input I_1 (say) will charge the capacitor C at a voltage equal to the peak of the analog pulse by means of high speed Op Amp IC-1 acting as a peak detector and is measured by the voltage follower IC-2. The drain current of transistor T_3 is normally cut off. The input pulse triggers IC-6 through transistor T_2 which produces a 3 μs width pulse. At the end of 3 μs, IC-7 is triggered to discharge the capacitor C by making transistor T_3 conducting. Thus the peak of each pulse is held for 3 μs during sampling.

As the "sample-and-hold input is held high during sampling 'enable controls' (E) of IC-10 and R_0 of IC-11 are also high so that IC-11 is at zero address and all the ouputs from the decoder (IC-10) are high. Thus all the outputs from S–H are cut off by the FET switch operating in the position T_4.

Normally, the control unit of the detector array where it is intended to be used contains TTL logic gates. The generation of a 'Hold Command' is almost instantaneous with the arrival of the selected pulses and hence falls within the sampling time of 3 μs. This 'Hold Command' makes R_D of IC-7, E of IC-10 and R_0 of IC-11 low; and at the same time it triggers IC-9 to produce a 2 μs width pulse. At the end of 2 μs, IC-8 is triggered to close all the input lines by making the input controlling transistor, in the position T_1, conducting. The width of the pulse from IC-8 must be greater than the time required for analysis. The input line is closed after 2 μs from the 'Hold Command' to ensure full peak value at the peak detector stage though it is operated by a fast operational amplifier. As R_D of IC-7 is low it will not trigger and the voltage across the capacitor C is retained. The wave form of the pulse after a "Hold" command is shown at the output of IC-2.

The "Hold" command connects the first channel to the output by making the output $\overline{O}$ of IC-10 low and counter (IC-11) ready for addressing the channels. All the 16 channels are analysed one after another by means of an ADC giving a channel advance instruction at the C_p input of IC-11.

During the whole cycle of operation, the input line is closed and therefore IC-6 will not be triggered which in turn keeps the "B" input of IC-7 high. The input "A" of IC-7 is permanently low. Hence, withdrawal of the hold command produces a low-to-high transition of R_D of IC-7. This transition of R_D when the "B" input is high and the "A" input is low triggers IC-7 to discharge the capacitor C.

5. Discussion

The "sample-and-hold" and analog multiplexer of the design described now is being operated in a cosmic

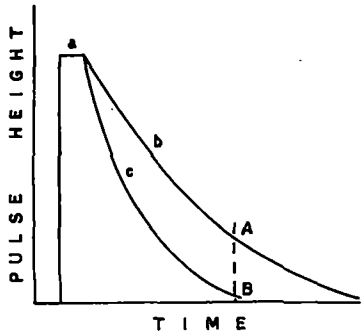

Fig. 2.Curve showing the discharge of the storage capacitor by a silicon transistor and a FET. (a) Width of the sampling pulse. (b) Discharge through the silicon transistor. (c) Discharge through the FET.

ray air shower experiment. The storage capacitor C should be large to avoid errors due to leakage when it is allowed to hold the voltage for a long time while an ADC scans all the voltages standing at 16 channels or even more when multiplexed. The optimum value of the capacitor is chosen at 0.02 μF to avoid "overshoot". During sampling the discharge of the capacitor C can be done by means of a silicon transitor by connecting its base directly to the Q output of IC-7 instead of using a FET. But with a silicon transistor the time of discharge of the condenser C is large compared to that for a FET as shown in fig. 2. The portion "a" in fig. 2 gives the width of the sampling pulse in an arbitrary scale and the two curves "b" and "c" give the discharge through a silicon transistor and FET respectively. At a particular time, indicated by the dotted line AB, if there is a "Hold" command when a high pulse is discharging after sampling, the "sample-and-hold" unit will hold the voltage present at that instant across the capacitor C by resetting IC-7. Thus by using a silicon transistor the channel will give information of voltage equal to the level A in the absence of any pulse in that channel. Therefore in a fast detecting system a FET is always preferable to a silicon transistor. A high slew rate operational amplifier 531 is used to multiplex the voltages to the output for making the voltage settling time minimum. It is observed that the voltage settling time of the analog multiplexer is less than 10 μs.

The authors acknowledge the provision of facilities including UGC Teacher Fellowships to G.C. Goswami and M.R. Goshdostidar and a Research Fellowship to B. Ghosh through the University of North Bengal, India.

The financial assistance received from the Department of Atomic Energy, Govt. of India, is thankfully acknowledged.

References

[1] A. Ogata, Nucl. Instr. and Meth. 115 (1974) 313.
[2] A.K. Chang and R.S. Larsen, IEEE Trans. Nucl. Sci. NS-20 (1973) 216.
[3] L.B. Robinson, F. Gin and H. Cingolani, Nucl. Instr. and Meth. 75 (1969) 121.
[4] M. Brossard and Z. Kulka, Nucl. Instr. and Meth. 160 (1976) 357.
[5] R. Bayer and S. Borsuk, Nucl. Instr. and Meth. 133 (1976) 185.

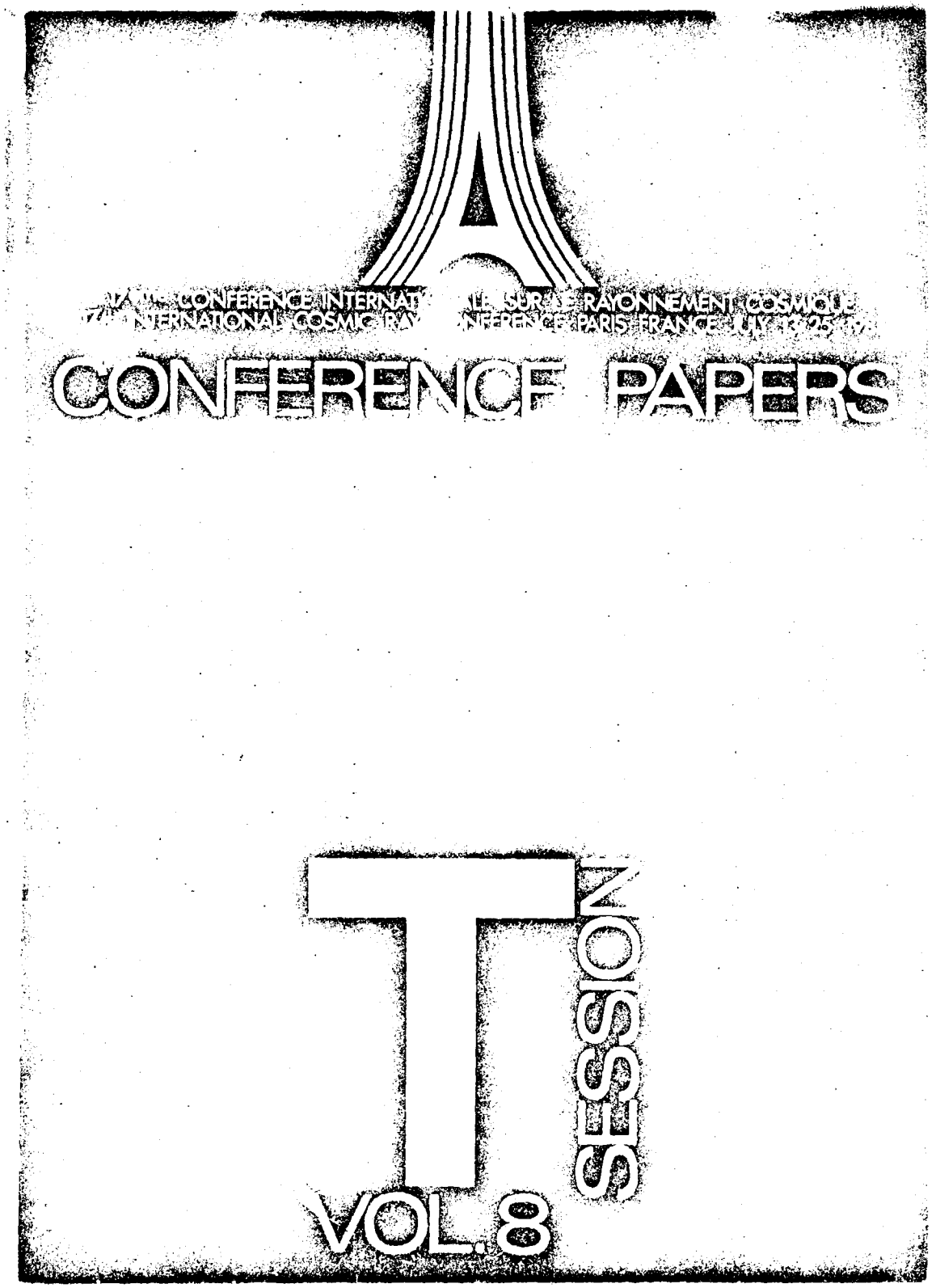
CONFERENCE INTERNAT
NTERNATIONAL COSMIC RA
LE SURSE RAYONNEMENT COSMIQUE
NFERENCE PARIS FRANCE JULY
CONFERENCE PAPERS
TOSES
VOL. 8

T 4-20

A PULSE HEIGHT RECORDING SYSTEM FOR SMALL AIR SHOWER ARRAYS

Goswami, G.C., Ghosh, B.
Ghoshdastidar, M.R.,
Basak, D.K.
Chaudhuri, N.
University of North Bengal
India

ABSTRACT

A pulse height recording system for a large number of channels from scintillation detectors of an air shower array has been designed, constructed and operated. In the present form of the system the digital output from individual channel is found to be linear upto 500 mV input. Each channel consists of a pre-amplifier, main linear-amplifier and a sample-and-hold. Each pulse height held by the sample-and-hold is scanned by the analog multiplexer and then digitised by an analog-to-digital converter. The digitised information is fed to a memory for printing on a paper tape.

1. Introduction

Analogue pulse from the array of detectors carrying particle density information is received by the pulse height analyser preconditioned by the selection system and operated by a master control unit. The block diagram as shown in figure 1 shows our present attempt to develop a system for recording pulse heights. The selected pulses are received, analysed and printed on a paper tape by means of a line printer.

2. Method

In the present form of the recording system, a pulse from each scintillation detector is amplified by a pre-amplifier consisting of operational amplifier of gain 20. The output pulse from pre-amplifier is further amplified by means of an amplifier of varying gain having an analogue switch at the input. Outputs from pre-amplifier and

amplifier are fed to sample and hold circuit, controlled by the master control unit. In the selection system, any three adjacent scintillators are taken to produce a coincidence master pulse to trigger the master control unit, cloud chamber control unit, Flash-tube-chamber control unit and Magnetic Spectrograph control unit. As soon as the master control unit is triggered it gives a hold command to the sample and hold circuit, switches off the input line, disconnects the coincidence circuit from the master control unit and sends a start-pulse to the programmed ADC and memory programme unit. The built-in-programme unit controlling the ADC, once triggered, connects all the pulses at the output of the sample and hold circuit by analog multiplexer one after another to the ADC for scanning. The digital outputs from ADC for each channel are de-multiplexed and displayed by seven-segment LED's for visual check and simultaneously recorded in a memory unit controlled by memory programme unit. The neon tube information of the magnetic spectrograph is received by a light sensing device which produces digital information. These output informations are stored in a memory unit.

The pre-amplifier and amplifier connected in our system are linear upto 10 V output. The output from the pre-amplifier is scanned to see whether there is any saturation at the output of the amplifier which will occur for large signal at the input. Since the pre-amplifier is of gain 20, the maximum voltage that can be recorded by scanning the pre-amplifier output by means of the ADC is 500 mV at the input point.

At the end of the ADC scan the memory programme unit produces a print command to the line printer and switches on the input line. The line printer first prints the digital pulse height and then the neon tube information of the magnetic spectrograph through a multiplexer controlled by the memory programme unit. At the end of the printing, the coincidence circuit is connected to the master control unit for the next event. The recording system of the cloud chamber and flash chamber are done by usual photographic method. Shower-frequency is recorded by connecting a scaler at the output of the coincidence circuit.

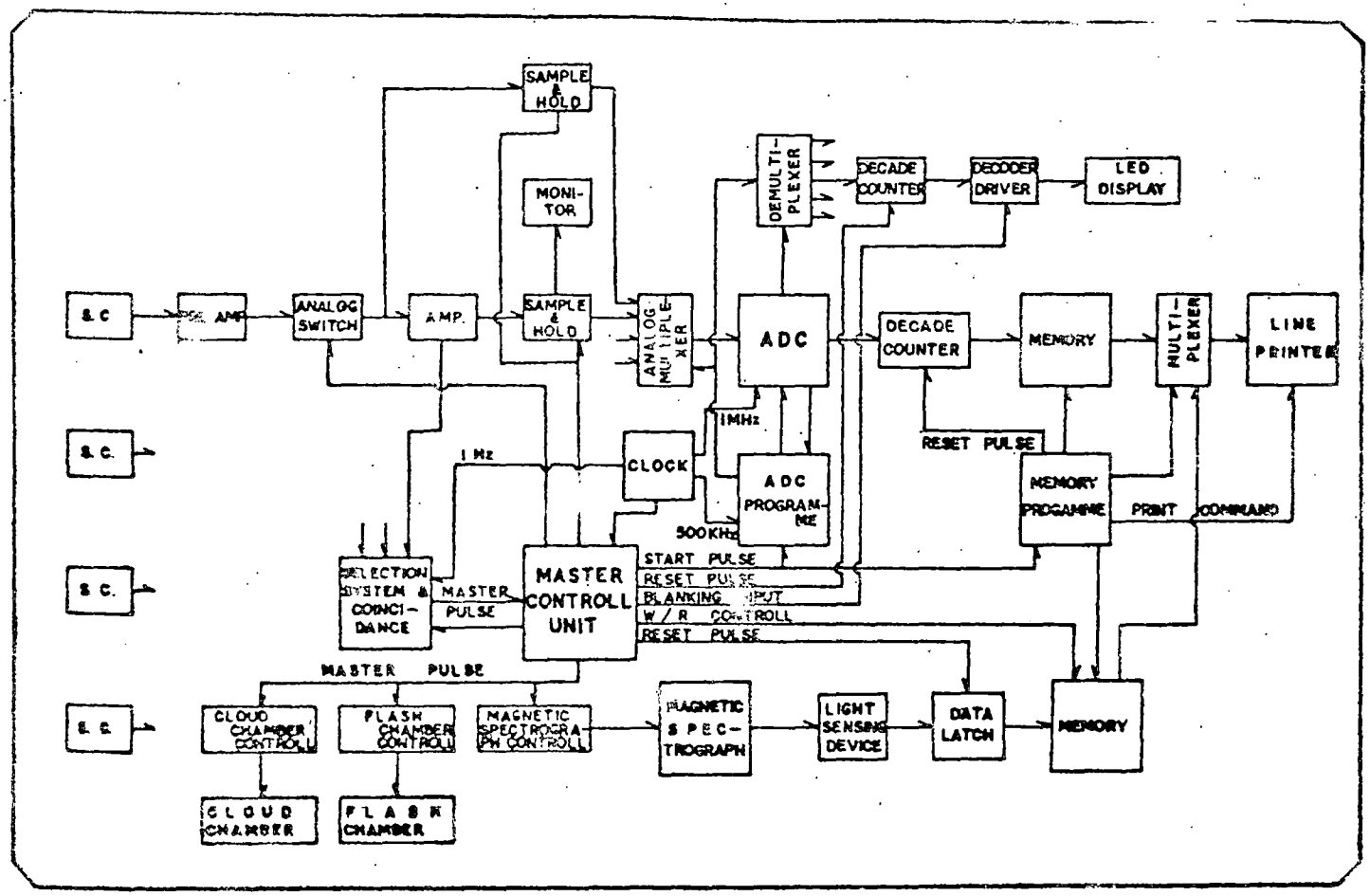

FIG. 1. BLOCK DIAGRAM OF ELECTRONICS OF AIR SHOWER ARRAY.


XVI
ICRC
KYOTO
1979

HADRON PRODUCTION IN INELASTIC MUON-NUCLEAR INTERACTION

G.C.Goswami, C.R.Paul*, N.L.Karmakar**,
A.Paul*** and N.Chaudhuri
Department of Physics, University of North Bengal,
India.

* P.M.Govt. College, Aizawl, Mizoram, India
** On leave to Kiel University, West Germany
*** A.C.College, Jalpaiguri, West Bengal, India.

ABSTRACT

The results of new measurements of the cross section for hadron production in muon-nuclear interactions by cosmic ray muons are presented. The nucleon structure function determined in recent deep inelastic lepton-nucleon scattering measurements using accelerator lepton beam has been used together with the Drell-Walecka formulation to calculate the cross section for hadron production in muon-nucleon interactions with large energy transfer but very small four-momentum transfer. A comparison of the calculation with the present and previous experiments is made to show the applicability of the method in cosmic ray experiments.

1. Introduction

The total cross section for hadron production by cosmic ray muons at high energies and accelerator muons at lower energies has been determined in a number of experiments. The cross section for hadron production in inelastic lepton-nucleon collision has been derived in terms of measured nucleon structure functions of Drell-Walecka formulation and the ratio of virtual photon cross sections. The calculated cross sections are used to evaluate the cross section data of our own measurements using cosmic ray muons and many other cosmic ray and accelerator measurements.

2. Derivation of the cross section

The inelastic lepton scattering cross section by nucleon, as given by Drell and Walecka, is expressed in the form

$$\frac{d^2\sigma}{d\nu\, dq^2} = \frac{4\pi\alpha^2}{(q^2)^2}\,\frac{E'}{E}\left[W_2(\nu,q^2)\cos^2\frac{\theta}{2} + 2W_1(\nu,q^2)\sin^2\frac{\theta}{2}\right] \qquad \ldots (1)$$

where E and E' are lepton energies before and after scattering at an angle θ by a nucleon of mass M, $W_2(\nu,q^2)$ and $W_1(\nu,q^2)$ are nucleon structure functions

$$W_1 = \frac{1}{4\pi^2\alpha}\left(\nu^2+q^2\right)^{1/2}\sigma_t(\nu,q^2) \qquad \ldots (2)$$

$$W_2 = \frac{1}{4\pi^2\alpha}\,\frac{q^2}{(\nu^2+q^2)^{1/2}}\left[\sigma_t(\nu,q^2)+\sigma_s(\nu,q^2)\right] \qquad (3)$$

where σ_t and σ_s are the absorption cross sections of transverse and scalar virtual photons by nucleons, $\nu = E-E'$ and q^2, the absolute value of the square of the four-momentum transfer from the lepton.

For extremely small scattering angle the scattering cross section can be reduced to the form

$$\frac{d^2\sigma}{dx\,dy} \cong \frac{4\pi\alpha^2}{2ME}\,\frac{F(x,q^2)}{x^2y^2}\left[1-y+\frac{y^2}{2(1+R)}\right] \qquad (4)$$

where

$$x = q^2/2M\nu \quad , \quad y = \nu/E$$

$$R = \sigma_s/\sigma_t = \frac{1.28\,q^2}{(q^2+1.16)^2}$$

and

$$F(x,q^2) \equiv \nu W_2(x,q^2)$$

The dependence of $F(x,q^2)$ on q^2 if $\nu \gg q^2$ as seen from eqn. (3) is of the form

$$\nu W_2(x,q^2) \equiv F(x,q^2) = \frac{q^2}{4\pi^2\alpha}\left[\sigma_t(\nu,q^2) + \sigma_s(\nu,q^2)\right] \qquad (5)$$

This has been checked by us by determining $F(x,q^2)$ as a function of q^2 taken in unit of M^2 from the recent accelerator data of e-N and μ-N scattering experiments. The result of this analysis is the following

$$F(x,q^2) = 1.24(q^2)^{1.06}\cdot 10^{-28} \quad (\text{cm}^2 \text{ per nucleon}) \qquad (6)$$

for $0 < q^2 < 0.1$; $0 < x < .02$

$$F(x,q^2) = 1.89(q^2)^{.73}\cdot 10^{-28} \quad (\text{cm}^2 \text{ per nucleon}) \qquad (7)$$

for $0.1 < q^2 < 0.5$; $.02 < x < 0.13$

Using these forms for $F(x,q^2)$ we have derived the differential and total cross section for hadron production both for a monoenergetic beam and for a cosmic ray muon beam. Some representative results are given in figure (1).

The expression obtained using eqn. (6) for differential and total cross section for muons of energy E are

$$\frac{d\sigma}{dy} = 1.36\left[\frac{1}{y} - 1 + \frac{y}{2(1+R)}\right] \quad \text{microbarn per nucleon} \qquad (8)$$

$$\sigma(>\nu,E) = 1.36\left[-0.7882 - \ln\frac{\nu}{E} + \frac{\nu}{E} - 0.2118\left(\frac{\nu}{E}\right)^2\right]$$

microbarn per nucleon (9)

For a cosmic ray muon beam with an energy spectrum $n(E)dE = AE^{-\gamma} dE$

$$\sigma(>\nu, >E) = 1.36\left[\ln \frac{\nu_{max}}{\nu} - \frac{(\gamma-1)\left(E_{max}^{-\gamma} - E^{-\gamma}\right)}{\gamma\left(E_{max}^{1-\gamma} - E^{1-\gamma}\right)} \left(\nu_{max} - \nu\right) \right.$$

$$\left. + \frac{(\gamma-1)\left(E_{max}^{-1-\gamma} - E^{-1-\gamma}\right)}{4(\gamma+1)(1+R)\left(E_{max}^{1-\gamma} - E^{1-\gamma}\right)} \left(\nu_{max}^2 - \nu^2\right) \right] \text{ microbarn per nucleon.} \quad (10)$$

The relative energy loss of muons of energy E due to this process is given by

$$-\frac{1}{E}\frac{dE}{dx} \equiv b_n = N \int_{y_{min}}^{1} y \left(\frac{d\sigma}{dy}\right) dy .$$

where N is the Avogadro number.

This quantity has been computed as a function of E for $\nu \geq 0.15$ GeV.

Table 1.
Comparison of computed values of $b_n (10^{-6}$ cm^2 per gm.) with experimental value.

Eqn. (6)			Eqn. (7)		Experimental value (1)
E(GeV)	10	1000	10	1000	
	0.514	0.525	0.142	0.142	0.57

The agreement between our calculated values of b_n in the first column of table 1 and measured values (see also Kobayakawa 1973) indicates improvement over earlier such computations (e.g. Kitamura 1977).

3. Experiment

In the late sixties, we started measurements (Paul et al 1975) on the production of knock-on electron, direct electron pairs, bremstrahlung and hadrons by cosmic ray muons in selected target materials in a multiplate cloud chamber operating first underground and then above ground in the oblique direction at 75° to the zenith. The multiplate cloud chamber (90 x 90 x 50 cms) containing Fe, Cu and Pb plates was triggered with the purpose of observing the various interaction events within it by single muons causing coincidence of multiple pulses from large area plastic scintillators. The chamber was in the shield of 200 g.cm^{-2} concrete. An iron target of thickness 316 g.cm^{-2} and a lead target of thickness 113 g.cm^{-2} were placed in the incident beam path for the production of hadronic showers. Another iron block, as the filter of produced particles, was placed below the chamber in between two scintillator counters.

4. Results and conclusion

4.1. Present experimental results - At 75° zenith angle operation of the apparatus, we observed 19 muon produced hadron production events due to 16.5 x 10^2 muon travarsals of two target producer layers in a time of 4.48 x 10^6 sec. The minimum energy transfer estimated is 3 GeV and total cross section is 1.75 ± 0.17 microbarn per nucleon for incident muons of mean energy 22 GeV. The contribution due to the incident nuclear active component at this oblique observation was estimated to be negligible. The results of other experiments with predicted cross section are given in fig.1

Figure 1

Comparis. with measured cross sections.

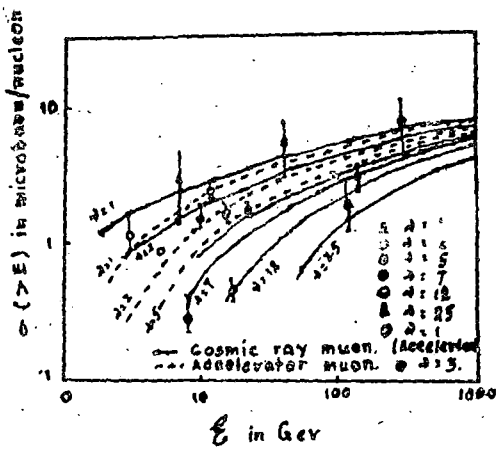

4.2. Comparison of results

For comparison with the measured cross section for hadron production by cosmic ray muons, the differential cross section, eqn. (3), has been averaged over the incident muon spectrum at each location of observation at sea level or underground. The exponent of the muon spectrum has been taken as 3.45(Sheldon et al 1973) above 100 GeV and 3 below 100 GeV. Minimum muon energy and energy transfer range for each experiment have been determined on the basis of the information available in the published papers. Maximum energy transfer, if not available, in the published papers, is determined from the relation

$$\nu_{max} = E - \frac{M}{2}\left\{\left(1+\frac{m^2}{M^2}\right)^2\right\}$$

where E is approximated to the average energy of the incident muon beam, m is muon rest mass.

The status of the measurements of hadron production by muons can be assessed from the comparison of fig. 1. The measured nucleon structure function $F(x,q^2)$ as given by eqn. (6), in q^2 interval 0-0.1 $(GeV)^2$, gives total cross sections consistent with 76% of the measurements, predicted cross sections remaining within the experimental error limits. The errors to the measured cross sections are large due to poor statistics of data in most of the experiments. In addition many of the experiments suffer from the uncertainties in identifying nuclear interaction events, estimation of energy transfer and lack of information on four-momentum range.

The structure function in the q^2 interval 0.1-0.5 $(GeV)^2$, as given by eqn. (7), predicts much lower cross sections in disagreement with measurements. The b_n values based on eqn. (6) showing

agreement of the measured result provides additional confirmation that cosmic ray muon-nuclear interactions involve q^2 values $\lesssim 0.1(\mathrm{GeV})^2$ even for interactions of energy transfer of the order of hundred GeV.

Thus the conclusion from all available cosmic ray measurements on muon-nuclear interaction process is that the structure function of eqn. (6) together with Drell-Walecka formula is adequate in explaining the phenomenon at all energy transfer if $q^2 \ll \nu$.

Acknowledgement

The authors acknowledge the provision of facilities including a U.G.C. Teacher-Fellowship to G.C.Goswami from the University of North Bengal.

References

1. Bezrukov et al 1972 Sov. J. Nucl.Phy. 15 313.
2. K.Kobayakawa 1973 Proc. 13th. Int.Conf. C.Ray. 5 3156.
3. Paul et al 1975 Proc. 14th Int.Conf. C.R. 6 1983.
4. Sheldon et al 1978 Phy.Rev. D 17 No. 1 p114
5. T.Kitamura 1977 Proc. 15th Int.Conf.C.R. 6 MN 113.

[illegible] INTERNATIONAL [illegible] CONFERENCE

[illegible]

[illegible]

[illegible]

[illegible]

[illegible]

MN 4-16

STUDIES ON DIRECT PRODUCTION OF ELECTRON-POSITRON PAIRS BY MUONS

A. Paul, N. L. Karmakar, B. Ghosh, M. R. Ghoshdastidar, G. C. Goswami and N. Chaudhuri.
Department of Physics,
University of North Bengal, Darjeeling, India.

ABSTRACT

The results of new measurements of the cross section for the direct production of electron-positron pairs by muons are presented, together with the predicted cross sections according to more recent calculation, to make a critical evaluation of the theory of the process.

1. Introduction.

The early experiments with cosmic ray electrons and muons gave an indication that the Bhabha (1935) or the MUT (Murota Ueda Tanaka, (1956) calculations were inadequate even in their ranges of applicability. In some of the later measurements, the total cross section of electromagnetic interactions (DPP, knock-on and bremsstrahlung) was determined and only in a few experiments, a separation of DPP events from knock-on and bremsstrahlung was attempted. We consider it useful to examine the present state of the theoretical DPP cross sections with the data of our earlier experiments and our new measurements. These are briefly described below.

(i) Chaudhuri and Sinha, (1964), Chaudhuri and Goswami (1970): DPP of electron-positron in thin and thick iron and lead targets by muons underground (mean energy 33 GeV) was studied in a multiplate cloud chamber.

(ii) Paul, Karmakar and Chaudhuri (1975): DPP events in thin targets of a multiplate cloud chamber operated at sea level in inclined directions (Zenith angle: 40-50 degree and 70-80 degree).

2. Results.

The reanalysed thin target (Fe) DPP data of our earlier measurements and the final thin target (Al, Cu, Pb) DPP data of new measurements are presented here. Theoretically expected results have been computed by taking into account the appropriate incident muon spectra and the DPP predictions according to the formulations of Bhabha (1935) and Kokoulin-Petrukhin (KP) (1970), being the representative calculations of CBb and QED treatments.

Table 1

Experimental values of DPP cross section (cm^2/g) from sea level measurements at three zenith angles.

(1)	(2)	(3)	(4)	(5)
SL,0°	6	Al,0.41	3-30	Expt: 6.8(2.1)-5
				KP : 5.7-5
				Bh : 5.5-5
SL,40°-50°	7	Al,0.41	3-30	Expt: 8.3(2.5)-5
				KP : 7.7-5
				Bh : 7.6-5
SL,70°-80°	24	Pb,1.7	3-30	Expt: 7.6(0.8)-4
				KP : 6.4-4
				Bh : 6.2-4
SL,70°-80°	24	Cu,1.3	3-30	Expt: 2.1(0.8)-4
				KP : 2.7-4
				Bh : 2.5-4
SL,70°-80°	24	Al,0.41	3-30	Expt: 1.0(0.4)-4
				KP : 1.5-4
				Bh : 1.4-4

(1) sea level zenith angle, (2) estimated mean energy of incident muons in GeV, (3) target element and thickness in $g.cm^{-2}$ (4) energy transfer range in MeV, (5) Cross-sections expected according to Kokoulin-Petrukhin (KP) (1970) and Bhabha (Bh) (1930) calculations compared with experimental results, (experimental error is in parentheses)

Table 2

Experimental DPP cross sections (cm^2/g) from measurements underground (depth 150 hg/cm^2)

(1)	(2)	(3)	(4)	(5)	(6)
UG,0	33	Fe,4.25	25-100	4.2(0.8)-4	3.9-4
			100-200	1.7(0.8)-4	1.3-4
			200-500	7.0(1.2)-5	9.9-5
			500-1,000	3.5(1.7)-5	4.9-5

(1) underground zenith angle, (2) estimated mean muon energy, (3) target element with thickness in $g.cm^{-2}$, (4) energy transfer in MeV, (5) experimental cross section (6) cross sections expected from the formulation of Kokulin-Petrukhin (KP) (1970)
The experimental data for relatively thicker targets of Fe and Pb covering energy transfer upto 16 GeV are not included in this presentation.

3. Conclusions.

The present evaluation shows that the version as given by Kokoulin-Petrukhin of the more exact QED calculations of the DPP of electron-positron process predicts cross sections almost the same as from the Bhabha calculation in the lower energy transfer range. The KP predictions are closer to MUT (alpha=1) predictions than to the predictions from MUT (alpha=2) calculation, particularly in the lower and intermediate energy transfer range. Difference between any two predictions in their appropriate energy range of validity is so small that they can not be distinguished by the existing cosmic ray muon and accelerator muon induced DPP measurements. The present results in the region of low energy transfer where only a few measurements have been conducted before, agree with theory. Thus we have the state of the DPP theory evaluated down to 3MeV energy transfer.

References.

1. Bhabha H.J. 1935 Proc. Roy. Soc. A 152 559; 1935 Cambridge Phil. Soc. 31 394
2. Chaudhuri N et al 1964 Nuvo Cimento 32 853
3. Chaudhuri N et al 1970 Nuovo Cimento A65 727
4. Kokoulin R.P. et al 1970 Proc. 11th ICRC Budapest; 1969 Acta Phy. Acad. Scien. Hung. 29 suppl 4 277; 1971 Proc. 12th ICRC Hobart. 6. 2436
5. Murota T et al 1956, Prog. Theo. Phy. 16. 382
6. Paul C.R. et al 1975 Proc. 14th ICRC Vol. 6 Munich 1963.

16TH INTERNATIONAL COSMIC RAY CONFERENCE

CONFERENCE PAPERS

VOL. 5

EA SESSIONS

XVI
ICRC
KYOTO
1979

KYOTO JAPAN

6-18 AUGUST 1979

A NEW AIR SHOWER PROJECT FOR STUDIES OF MUONS AND HADRONS

N.Chaudhuri, B.Ghosh, M.R.Ghoshdastidar
and G.C.Goswami
Department of Physics,
University of North Bengal,
Darjeeling, India.

ABSTRACT

The new air shower project at NBU using the Department of Atomic Energy Magnetic Spectrograph for momentum measurement of muons upto a thousand GeV/c will be reported. The aim is to study (i) momentum spectrum and charge ratio of air shower muons (ii) energy spectrum and charge ratio of air shower hadrons and (iii) electromagnetic interaction of muons.

1. Introduction

The new project for making observation on air showers at ground level has been undertaken at the University of North Bengal. The main aim is to study the muon component and the hadron component in the same air shower in 'direct experiments' using a Magnetic Spectrograph and visual detectors.

2. The experimental arrangement

The investigation will be carried out by using an air shower array of plastic scintillator detectors, a Magnetic spectrograph for the momentum measurement of muons near the centre of the array, a large volume neon flash tube chamber for observation of muons away from the centre of the array and a multiplate expansion chamber as the detector of hadrons near the centre of the array.

2.1. The air shower array

The air shower array is based at the initial stage on 13 plastic scintillator counters, spread over a diameter of 12 m,

Figure 1
Air Shower Array

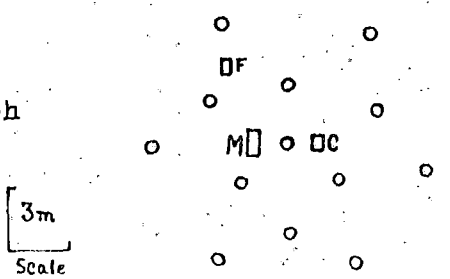

as electron density detectors in an incident air shower. The lay-out of the detectors is shown in fig. 1. The response of the array has been tested. The minimum shower size detectable by the array has been determined to be in the range $1 \times 10^5 < N < 2 \times 10^5$

2.2. The muon detector

The magnetic spectrograph (Fig. 2) having a maximum detectable momentum of $\sim$ 1000 GeV/c and an acceptance solid angle $\sim$12 cm^2.sr. will be combined with neon flash tube trays to locate the path of muons for momentum measurement. The spectrograph is triggered by a G M Counter telescope in coincidence with the air shower array.

A multilayer neon flash tube chamber (2x2x1.5m) with a 5 cm. of lead shield on the top will be placed at about 5 metre from the centre to detect the low energy muons in an incident shower.

Figure 2
Front view of one limb of magnetic spectrograph. Plan of magnetic spectrograph assembly.

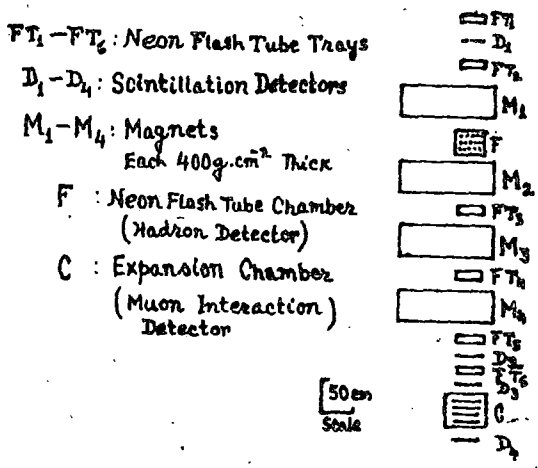

2.3. The hadron detector

A multiplate expansion chamber of dimensions (1mX1mX50 cm.) with 12 iron plates each of 2 cm thickness will be located near the centre of the array to detect the hadrons in the air shower. The chamber will be shielded at the top by 2.5 cm. of lead. The hadron detector will be triggered by a G M Counter telescope in coincidence with the air shower array. The threshold energy of the hadron detector is adjustable in the present arrangement (Fig. 3).

Figure 3
G M Counter Telescope

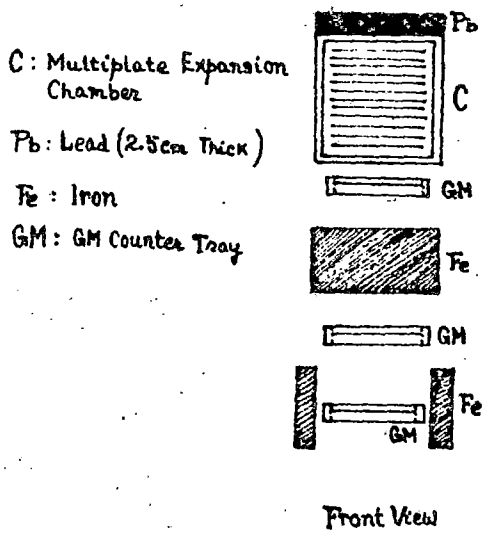

3. Possible measurements

The combination of the Magnetic spectrograph combined with a multiplate cloud chamber at its bottom, a multilayer flash tube chamber and another multiplate expansion chamber as hadron detector will make it possible to measure (i) the momentum spectrum of muons (ii) the charge ratio of muons (iii) the energy spectrum of hadrons, (iv) the charge ratio of hadrons and (v) the interaction processes induced by very high energy muons in a visual detector.

17ème CONFERENCE INTERNATIONALE SUR LE RAYONNEMENT COSMIQUE
17th INTERNATIONAL COSMIC RAY CONFERENCE PARIS FRANCE JULY 13-25 1981

CONFERENCE PAPERS

HE SESSION

VOL. 5

HE 1.1

A CRITICAL EVALUATION OF THE SINGLE PARTICLE INCLUSIVE CROSS SECTIONS USED FOR DESCRIBING PARTICLE PRODUCTION IN HIGH ENERGY COSMIC RAY INTERACTIONS

Ghoshdastidar M.R., Goswami G.C.
Ghosh B., Basak D.K.
Chaudhuri N.
University of North Bengal
India

ABSTRACT

Various single particle inclusive cross section formulae which have recently been used in the calculations of cosmic ray cascading have been critically examined. This evaluation reveals the degree to which the various forms of cross section representations show unity in their predictions and with currently available more accurate cross sections at higher energies.

1. Introduction

Recently many attempts have been made to interpret very high energy nuclear interaction processes in extensive air showers and to relate the sea level muon spectrum and the charge ratio with primary cosmic ray spectrum by making use of the available data on inclusive cross sections in hadron collisions in the limited accelerator energies. In these papers the cross sections have been extrapolated to cosmic ray energies assuming scaling behaviour in the data. The predictions of these papers differ widely. This is due to (i) the use, in some early papers, of preliminary lower energy data (ii) a variety of forms used to represent the same data for use in calculation of cosmic ray cascading at very high energies and (iii) lack of data in certain regions of produced particle-kinematics. Consequently, the present status of such interpretative work is that despite many attempts the situation in this area of interest remains unsolved. The various inclusive cross section representations appear to deserve a presentation which will exhibit the degree to which the various forms of cross sections show unity in their predictions and with currently available more accurate data at higher energies. Such a presentation has been attempted by critically evaluating sever-

al of the important forms of cross sections which have been used in the calculation of cosmic ray cascading.

2. Inclusive cross sections

The cross sections determined over a wide range of accelerator energies for various inclusive hadronic reactions for production of particles (pion, kaon, antinucleon) are usually expressed in Feynman approach in centre of mass system (C.M) in variable x(x_F, Feynman scaling variable; or x_R, Yen or radial scaling variable) and p_t, transverse momentum.

In the alternative approach of Yen et al (1974) the variable y (laboratory longitudinal rapidity) and p_t are used to express the cross section data. In the Feynman (1969) approach, the cross section function $f(x,p_t, \sqrt{s})$, (s, squared C.M energy) when plotted as a function of x is predicted to show at sufficiently high energy s, the behaviour

$$f(x,p_t, \sqrt{s}) \rightarrow g(x,p_t) > 0$$

In the approach of Yen, the invariant cross section plotted as a function of y is predicted to show at high energy s the behaviour

$$f(y, p_t, \sqrt{s}) \rightarrow g(y, p_t) > 0$$

The cross section data measured in various ranges of these variables and beam energy have been investigated by many authors to examine the dependence on these variables in the limited range of s. The various representations thus obtained and published are listed and described below.

3. Differential cross section's form

The usual method adopted to examine if the cross sections for a given x and p_t at a fixed $\sqrt{s}$ for production of a certain secondary particle in a hadronic inclusive reaction becomes independent of $\sqrt{s}$ at high s is to plot the cross-sections as a function of x for various values of p_t and to obtain a single function in x and p_t for all beam energies. In an alternative procedure the data are plotted as a function of p_t for several x values to obtain a single function in x and p_t. In most of the published papers the cross section data have been found to be only qualitatively s-independent over the limited ranges of x and beam energy studied and available so far. The form-fits thus obtained have been used in many calculations of cosmic

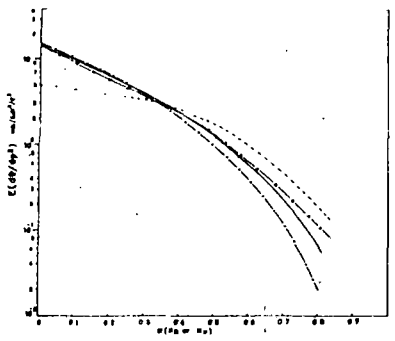

Fig. 1. Plot of invariant cross sections according to various formulations for the reaction $p+p \rightarrow \bar{\Lambda}^{+} +$ anything.

---- Ref(6); —x— Ref(4); — Ref (5) —·— Ref (1)

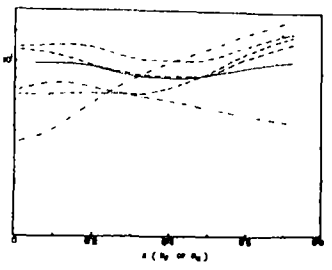

Fig. 2. Plot of R, the ratio $x(d/dx)$ cross sections according to various formulae, for the reactions $p + p \rightarrow \pi^{+}$+anything. —···— Ref (6); --- Ref (7); —·— Ref (8); ···— Ref (1); —— Ref (2); ------- Ref (4).

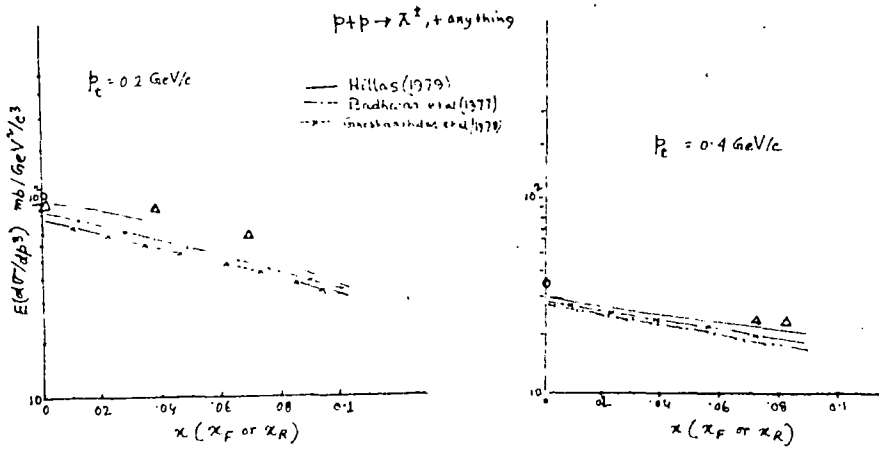

Fig 3. Comparison of single particle inclusive cross sections with data △ Fanvini et al (1972) . o Guettler et al (1976)

ray cascading[a1] given in the following

1. Erylkin et al (1974): $p + p \to \pi^{\pm}, K^{\pm}$ + anything; $0.05 < x_R < 1$ $0.2 < p_t < 0.8$ GeV/c; $\sqrt{s} = 44.6$ GeV
2. Badhwar et al (1977) $p + p \to \pi^{\pm}, K^{\pm}$ + anything; $0 \leq x_R < 1$; $0.2 < p_t < 0.8$ GeV/c; beam energy: 6 -1500 GeV
3. Thompson et al (1977) : $p + p \to \pi^{\pm}, K^{\pm}$ + anything; $0 \leq x_F < 1$; $0.2 < p_t \leq 0.8$ GeV/c; beam energy 24-1500 GeV
4. Johnson et al (1978): $p + p \to \pi^{\pm}, K^{\pm}$ + anything; $0 < x_R < 0.8$ $0.25 < p_t < .75$ GeV/c; beam energy: 100-400 GeV
5. Ghoshdastidar et al (1978): $p + p \to \pi^{\pm}, K^{\pm}$ + anything; $0 < x_F < 1$; $0.2 < p_t < 8$ GeV/c; beam energy 6-2000 GeV
6. Volkova et al (1979): $p + p \to \pi^{\pm}, K^{\pm}$ + anything; $0 \leq x_R < 1$ beam energy: 6-1500 GeV.
7. Hillas AM (1979): $p + p \to \pi^{\pm}, K^{\pm}$ + anything; $0 \leq x_R < 1$; $0.2 \leq p_t \leq .8$ GeV/c; beam energy: 10-2200 GeV.

4. Numerical computation of the cross sections

All the important parametric representations for the inclusive cross sections have been computed using the values of the parameters as given by the respective authors. A selection of computed results is given in Fig. 1.

To show the differences in the predicted cross sections according to various formulae, have been integrated over p_t and then the results ($x \frac{d\sigma}{dx}$) are plotted in figure (2) relative to that from Hillas (1979). Over the whole regions of x considered the predictions of the various formulae diverse strongly indicating that the experimental data represented in parametric form only in terms of x_R and p_t over the limited range of s investigated so far are perhaps inaccurate and incomplete.

References

1. Badhwar GD et al 1977 Phy Rev D15, Vol 3 p820
2. Erlykin AD et al 1974 J.Phy A7 2059
3. Feynman RP 1969 Phy Rev. Lett 23, 1414
4. Ghoshdastidar MR et al 1979 Il Nuv. Cim. Vol 1C Ser 1 No 5 p439
5. Hillas AM 1979 Proc. 16th ICRC EA 3-3 p13
6. Johnson IR et al 1978 Phy Rev. D17 p1292
7. Thompson MG et al 1977 J.Phy G Vol 3 No. 1 p97
8. Volkova et al 1979 Sov. J.Nucl. Phy. 29(5) p645
9. Yen E 1974 Phy Rev. D10 p 816
10. Panvini RS et al 1972 Phys. Lett. 38B, 55
11. Guettler K et al 1976 Phys. Lett. 64 B, 111

17ème CONFÉRENCE INTERNATIONALE SUR LE RAYONNEMENT COSMIQUE
17th INTERNATIONAL COSMIC RAY CONFERENCE PARIS FRANCE JULY 13 25 1981

CONFERENCE PAPERS

MN SESSION

VOL. 7

MN 4-11

NUCLEAR SHADOWING IN LEPTOPRODUCTION AND PHOTOPRODUCTION OF HADRONS

Ghosh B., Ghoshdastidar M.R.,
Basak D.K., Goswami G.C.
Chaudhuri N.

University of North Bengal
INDIA

ABSTRACT

New measurements of nuclear shadowing in leptoproduction and photoproduction of hadrons representing improvement in precision over earlier such experiments have been subjected to a critical analysis to examine their energy dependence and dependence on mass number. Several of the published calculations on nuclear shadowing have been considered by finding their predictions and by indicating the differences in their predictions and between predictions and measurements of shadowing in nuclear muoproduction, electroproduction and photoproduction of hadrons.

1. Introduction

Inelastic muon-nucleus (A) and electron-nucleus scattering measurements provide total photonuclear cross section ($\sigma_{\gamma A}$) for virtual photons. The photon shadowing 'S' in target nuclei expressed as ($\sigma_{\gamma A}/A\sigma_{\gamma N}$) (effective fraction of nucleons in the nuclear target) can thus be determined as a function of virtual photon energy E_γ and the square of four-momentum transfer q^2. The measurements of total cross-section for hadron production by inelastic lepton-scattering yield the effective fraction of nucleons in a nuclear target at very small q^2 -values but over a wide virtual photon energy range. These data together with the data from the real photoproduction experiments are taken together for testing existing calculations on nuclear shadow effect. Old experimental data on nulcear shadowing from real photoproduction experiments and also electroproduction experiments contain large uncertainties. New experimental data represent great improvement in the precision of measurements and appear to deserve a presentation which will exhibit a relation between various theoretical

predictions. In this paper, we attempt such a presentation considering the experimental data from recent measurements and latest theoretical predictions.

2. Nuclear shadow-effect calculations

The theory of shadowing of real and virtual photons in nuclei is based on

i) vector-meson dominant model in which photons are assumed to interact with nucleons via vector mesons.

ii) many-channel hadron-dominant model (generalised vector dominant model) in which photons are assumed to interact with nucleons via hadron states.

The pure 'Rho-dominant' calculation of photon shadowing has been given among others by Brodsky and Pumplin (1969). The multi-channel shadow-effects have been calculated neglecting off-diagonal elements between hadronic channels by Brodsky and Pumplin (1969). In the refined calculations of Cocho et al (1974), Distas et al (1975), Bezrukhov and Bugaev (1979), these off-diagonal terms have been shown to be significant in the case of heavier nuclear targets. The predictions of these calculations have not yet been mutually compared and tested adequately using reliable experimental data from shadowing of real and virtual photons in heavier nuclei.

3. Experimental data and analysis

We propose to examine photon shadowing through a study of (a) photon energy dependence on some target nuclei (A) and also (b) A-dependence for some photon energies using data from (i) cosmic-ray muon-nucleus inelastic scattering experiments (ii) accelerator electron-and muon-nucleus scattering experiments and (iii) real photoproduction experiments. The cosmic ray muon experiments provide total photonuclear cross-section at very low q^2 (≈ 0) values over a wide virtual photon energy range. Experiments so far reported on inelastic electron-scattering and muon scattering have provided data at low q^2 values and have been combined with cosmic ray muon data for this analysis is based on

i) Measurements for virtual photons by

a) Lanin et al (1971)
b) Heynen et al (1971)
c) Paul et al (1975)

d) Eickmeyer et al (1976)
e) Baily et al (1979)

ii) Measurements for real photons by

a) Brooke et al (1973)
b) Daresbury report (1973)
c) UCSB report (1973)
d) Michalowski et al (1977)
e) Gabathuler E (1978)

To examine the data on the energy dependence and A-dependence, the data points with $q^2 \lesssim 0.1$ are plotted as a function of photon energy E_γ on some nuclei as shown in Fig. 1, and plotted as a function of A for several photon energies as shown in Fig. 2. The results are presented as fitted curves that represent the data well. The dependence of the data on A and E_γ is obtained in the form:

$$\sigma_{eff}/A) = 0.65 + 0.48A^{-.07} \cdot E_\gamma'^{-.49}, \quad E_\gamma' \text{ in unit}$$

of nucleon rest mass.

4. Comparison with theoretical predictions and conclusion

The theoretical predictions according to several of the calculations are displayed in fig. 3. Predictions of Brodsky and Pumplin (1969) above a photon energy of 5 GeV are higher than experimental data and those from the predictions of Distas et al (1975). The dependence of the shadowing on photon energy is seen to be very week. The shadowing observed in real photoproduction experiments is found to show a behaviour in qualitative agreement with that observed in low q^2 leptoproduction process.

References

1. Bezrukov and Bugaev 1979
2. Brodsky SJ and Pumplin J : 1969 Phy Rev. Vol. 182 No. 5 p 1794
3. Baily et al 1979 Nucl. Phy B 151 p 351
4. Brookes et al 1973 Phy Rev. D8 p2826
5. Cocho G et al 1974 Nucl. Phys. B78 p269
6. DESY report 1971 Physics Lett. 34B p651
7. Distas P et al 1975 Nucl. Phys. B99 p85
8. Eickmeyer J et al 1976 Phy Rev Lett Vol 36 No. 6 p289
9. Gabathuler E 1978 Proc. 19th Int. Conf. High Energy Physics;
10. Heynen V et al 1971 Phy Lett 34B p651
11. Lakin WL et al 1971 Phy Rev Lett Vol 26 p34
12. Michalowski S et al 1977 Phy Rev Lett Vol 39 No,12 p737
13. UCSB report 1973 Phy Rev D7 p1362
14. Paul A et al 1975 Proc. 14th Int. Conf. C. Ray, Munich, 1983

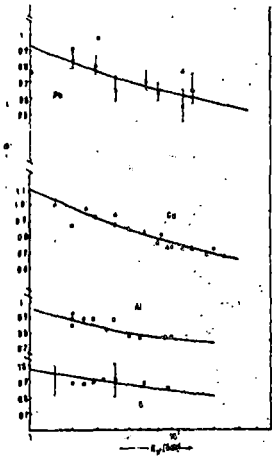

Fig. 1 (A_{eff}/A) vs E_r presented as fitted curves for various values of A. Data points from Refs. 3,4 & 8-13

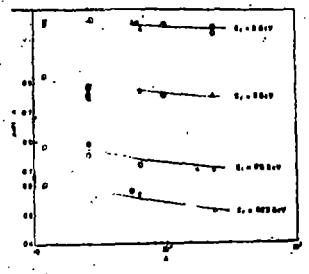

Fig. 2 (A_{eff}/A) vs A presented as fitted curves for various values of E_r. Data points from Refs. 3,4 & 8-13.

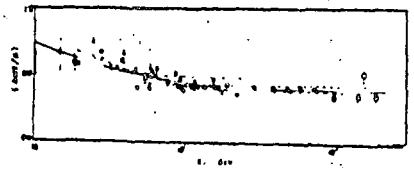

Fig. 3 (A_{eff}/A) for copper target compared with various theoretical predictions: — · — Ref.(1); — : — Ref(5); - - - - Ref(1); —— Present work. Data points from Refs. 3,4 & 8-13.